First

PROGRESS REPORT

(Project SR-108)

on

CRITICAL STRESS FOR SLIP, TWINNING, AND CLEAVAGE IN SINGLE CRYSTALS OF IRON

by

J. J. Cox, Jr., G. T. Horne and R. F. Mehl
CARNEGIE INSTITUTE OF TECHNOLOGY

Transmitted through

**NATIONAL RESEARCH COUNCIL'S
COMMITTEE ON SHIP STEEL**

Advisory to

SHIP STRUCTURE COMMITTEE

May 15, 1953

SHIP STRUCTURE COMMITTEE

MEMBER AGENCIES:

BUREAU OF SHIPS, DEPT. OF NAVY

MILITARY SEA TRANSPORTATION SERVICE, DEPT. OF NAVY

UNITED STATES COAST GUARD, TREASURY DEPT.

MARITIME ADMINISTRATION, DEPT. OF COMMERCE

AMERICAN BUREAU OF SHIPPING

May 15, 1953

Dear Sir:

As part of its research program related to the improvement of hull structures of ships, the Ship Structure Committee is sponsoring a study of critical stress for slip, twinning, and cleavage in single crystals of iron at Carnegie Institute of Technology. Herewith is a copy of SSC-59, First Progress Report on Project SR-108, entitled "Critical Stress for Slip, Twinning, and Cleavage in Single Crystals of Iron", by J. J. Cox, Jr., G. T. Horne and R. F. Mehl.

The project is being conducted with the advisory assistance of the Committee on Ship Steel of the National Academy of Sciences-National Research Council.

Any questions, comments, criticism or other matters pertaining to the Report should be addressed to the Secretary, Ship Structure Committee.

This Report is being distributed to those individuals and agencies associated with and interested in the work of the Ship Structure Committee.

Yours sincerely,

K. K. COWART
Rear Admiral, U. S. Coast Guard
Chairman, Ship Structure Committee

First
PROGRESS REPORT
(Project SR-108)

on

CRITICAL STRESS FOR SLIP, TWINNING, AND CLEAVAGE

IN SINGLE CRYSTALS OF IRON

by

J. J. Cox, Jr.
G. T. Horne
R. F. Mehl

CARNEGIE INSTITUTE OF TECHNOLOGY
METALS RESEARCH LABORATORY

under

for

SHIP STRUCTURE COMMITTEE

TABLE OF CONTENTS

LIST OF FIGURES

CRITICAL STRESS FOR SLIP, TWINNING, AND CLEAVAGE
IN SINGLE CRYSTALS OF IRON

Introduction

Whether the low temperature brittleness of steel and the
brittle fracture characteristics of ship plate can be corre-
lated with a true ductile-to-brittle transition in pure iron
has long been a question in the minds of engineers and metal-
lurgists. If such a correlation exists, can the transition
phenomenon be eliminated or raised by heat treatment or alloy-
ing additions? This and other questions can only be answered
by experiments that examine the modes of deformation in single
crystals.

A survey of existing literature reveals many experimental
studies of deformation of single crystals of hexagonal and
face-centered-cubic metals. Zinc, cadmium, aluminum, copper,
and alpha brass have been studied extensively, and values of
the shear stress required to initiate slip and twinning have
been obtained at various temperatures for the several metals.
The traces of the glide or twin planes upon the polished
surface of the specimens were used to determine the crystal-
lographic plane of deformation. These traces were lines
which outlined one or more sets of low index planes and direc-
tions. In the hexagonal metals, the glide plane was the
(0001) and the glide direction the $[2\bar{1}\bar{1}0]$. The face-centered

metals and alloys exhibited glide planes of the (111) type
and [10$\bar{1}$] directions--again the plane of highest atom density
and the closest packed direction. Some variation in the
glide plane occurred with changes in temperature, state of
stress, and manner of loading; but in all cases the direction
of closest packing was operative.

If the body-centered lattices were to deform in a similar
manner, the predicted glide plane should be the (110) and the
direction the [111]. However, metallographic specimens of
α-iron deformed in compression at room temperature showed
forked and wavy slip lines which indicated no single crystal-
lographic plane. This initial observation led to several inves-
tigations on the mechanism of deformation in alpha iron.

In 1926 Taylor and Elam[1] tested small single crystals
of relatively pure ferrite in both tension and compression.
A rectangular grid work was engraved on the polished surface
of the specimens, and the subsequent change in shape of the
rectangles upon deformation enabled the investigators to
calculate the plane and direction of slip. They concluded
that the glide plane either coincided with or lay near the
plane of maximum shear stress containing the [111] direction.
Since the pole of the glide plane sometimes fell between two
planes of low index, the authors proposed a theory of non-
crystallographic or "banal" glide. Taylor and Elam also

considered multiple slip on non-parallel planes containing the [111] direction, thus giving a wavy effect to the slip lines but discarded this explanation in favor of the banal mechanism.

In 1928 Taylor[2] continued his work on the body-centered-cubic structure using beta brass and observed that the results were quite similar. One exception, however, seemed significant. In iron, when the pole of the glide plane did not coincide with a low index plane, it was always inclined away from the maximum shear stress pole toward the nearest (112) plane containing the slip direction; but in beta brass, the glide plane poles were always inclined toward the nearest (110) pole. On the basis of his observations, Taylor derived an equation relating the resistance to shear of a given plane to its position in the (111) zone:

$$F = \frac{P}{A} \cos \xi \quad \sin \xi \quad \cos (X - \psi).$$

where   F = shear resistance

A = area of specimen

P = yield point load

ξ = angle between slip direction and specimen axis

X = angle between maximum shear plane and closest
(110) plane (both containing the slip direction)

ψ = angle between slip plane and closest (110) pole.

By differentiation, and integration between the limits 0 and ψ, a relationship was obtained which enabled Taylor to calculate the ratio of the resistance to shear of any plane in the zone to

the resistance to shear of the (110) plane. Since this cal-
culation produced a curve of resistance to shear versus ψ
similar to that predicted by the banal mechanism, Taylor was
convinced that this was correct. It does not seem likely
that the body-centered lattice should differ so radically in
its deforming characteristics from all other lattices.

Some four years later, Fahrenhorst and Schmid[3], in
Germany, studied the plastic flow of iron crystals by more
or less indirect observation. They obtained orientation
measurements of their crystals but used no grids and measured
no glide traces. Instead, they assumed that there were four
possible planes on which slip could occur:

1. On the (110) plane

2. On the (123) plane

3. On the (112) plane

4. On the maximum shear stress plane.

They concluded that the systems (123): [111] explained the
observations. Measurements of shear stress and shear strain
strengthened their belief in this mechanism since the scatter
or variation in results was less for this system than for the
others.

These conclusions are not necessarily correct for the
variation in the data; assuming any of the four systems to
operate leads to results which are equal within the limits
of experimental errors.

However significant the conclusions, this work produced
a simple method for the determination of the slip direction
from the migration of the specimen axis during deformation.
Two or more Laue photograms are taken at successive stages
in the extension or compression of the crystal and the
stereographic projections of these pictures are superimposed.
A line drawn through the load axes at the different stages
intersects the pole of the slip direction. A few exceptions
were found, but in general the slip direction was [111] .

Barrett, Ansel, and Mehl[4], of this laboratory, exam-
ined the deformation mechanisms of single crystals of iron
and silicon ferrite at several temperatures using sheet
specimens of single crystal material. The trace normal
method described by Barrett[5] was used to determine the
slip plane and in every instance the glide plane could be
explained by one of the planes (110), (112), or (123) within
the limits of accuracy of the method. Since it was implicitly
assumed that slip was crystallographic in the [111] zone, the
results are not so conclusive as one might be led to believe.

Twinning and cleavage were also studied in this inves-
tigation. The twin system was found to be (112): [111] and
the cleavage plane the (100). In the alloyed crystals, in-
creasing the silicon content tended to:

1. Increase the temperature at which twinning occurred.
2. Increase the frequency of slip on the (110) [111] system.
3. Decrease the waviness of the slip lines.

Schematic curves of critical resolved shear stress for slip
and twinning and critical normal stress for cleavage as a
function of temperature were plotted (see Fig. 1).

Andrade[6] stated that the testing temperature deter-
mines the operative glide plane and on this basis calculated
ratios of test temperature to melting point for several metals.
This criterion is not adequate except for the alkali metals
since several slip planes are found on a single specimen.
Smoluchowski[7] proposed that the ionic core repulsion in
non-alkali metals may qualitatively account for their
deviation from the Andrade relationships.

Opinsky and Smoluchowski[8,9] stated that the slip system
is determined by the position of the specimen in the unit ster-
eographic triangle, as shown in Fig. 2. These areas or regions
are calculated assuming that the shearing strength of the (110),
(112), and (123) planes are equal. The authors pointed out
that this may not be true but that there are no data upon which
to base a different approach. Again it is implicitly assumed
that the glide ellipse is both macroscopically and microscop-
ically a true atomic plane.

Chen and Maddin[10] explored the nature of slip in single
crystal wires of molybdenum and found the pole of the glide
ellipse to vary along the [111] zone. Their picture was one of
cooperative slip on planes of the (110) type. Segments of vary-
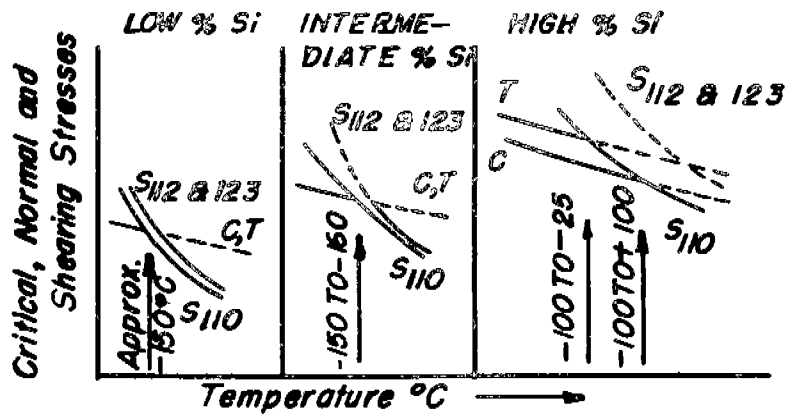ing length of two (110) planes could form slip lines with poles

Fig. 1

Critical Resolved Shear Stress versus
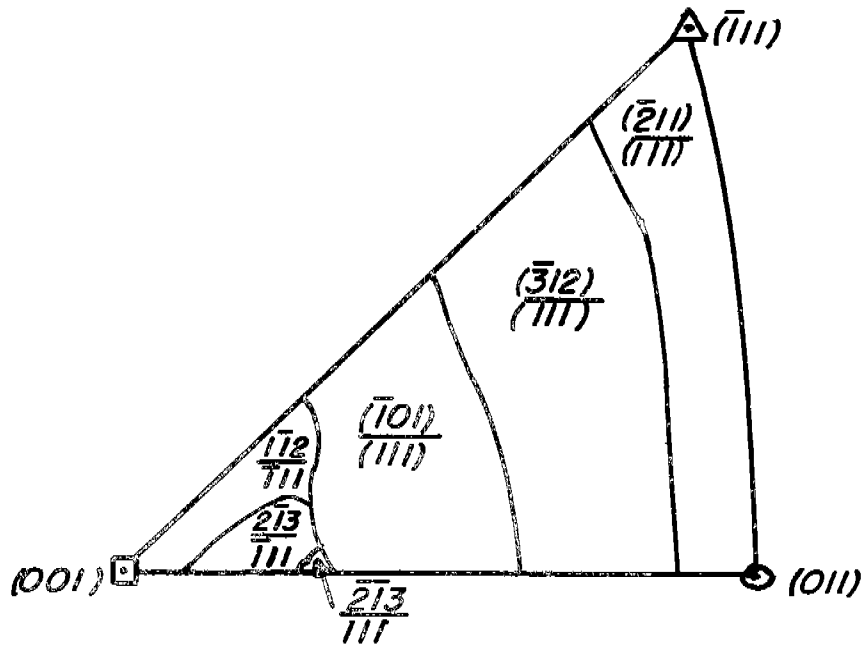Temperature. (After Barrett, Ansel and
Mehl)

Fig. 2

Regions of highest resolved shear stress
in the unit stereographic triangle. (After
Opinsky and Smoluchowski)

lying anywhere along the [111] zone. Brick and Vogel[11], in the discussion to this paper, suggest that when the pole of the integrated glide ellipse coincides with a (110) pole, the trace of this ellipse should be straight at any azimuthal position on the surface of the specimen. If, perhaps, cooperative slip on (112) or (123) was the mechanism, then this is not a valid objection. Maddin points out also that lattice rotation could account for this behavior.

The data of all investigators appear to be quite similar, but the explanations differ quite markedly. It is true that a mechanism involving high index planes does not seem plausible, for the shearing strengths of these planes are expected to be quite high; yet the experimental results indicate that the wavy slip lines are not in every case explained by cooperative shear on low index planes. The failure of all proposed mechanisms to explain the observations are related in a common fault--insufficient resolving power. The real need in any case is for a new tool to detect the plane or planes of slip on an atomic scale rather than on a microscopic one. Our techniques are too crude by several orders of magnitude.

The method of attack of this investigation was to measure the glide traces of single crystals and resolve the stress at yielding onto the glide plane. The super-complex nature of slip in iron was not anticipated as causing trouble in a stress measuring experiment within the accuracies required, and

consequently a tangential course into the realm of deformation mechanistics was not plotted. However, since the work of Brick and Vogel and Chen and Maddin, plus the early results of this project, have indicated the importance of resolving the complex nature of slip in iron, the original plans have been somewhat modified. The objectives of this investigation reported herein are as follows:

1. To produce a ferrite of nominal purity from SAE 1008 steel.

2. To grow single crystals of this material of a size suitable for subsequent tension tests.

3. To find the critical resolved shear stresses for slip and twinning insofar as they can be determined as a function of temperature.

4. To determine whether a transistion from slip to twinning occurs with repoducibility of results and whether a criterion for the onset of twinning can be established.

5. To study the fracture properties of single crystals as a function of temperature, strain, aging, and prestrain.

6. To investigate the atomic nature of slip in iron by methods of higher resolving power, e.g.,

    a. The electron microscope.

    b. Multiple beam interferometry.

7. To correlate the above in a general theory of
   deformation for α-iron.

Experimental Techniques

The ideal material for producing single crystals of re-
latively pure iron would be a vacuum melted high purity iron
such as Westinghouse "Puron" or National Research Corporation
pure iron. Preliminary experiments failed to produce a suc-
cessful strain anneal cycle for single crystal production.
Several shapes and sizes of specimens were tried but with
little or no success. It was believed that the variation in
properties of the irons from batch to batch prevented the data
from one heat of iron being applicable to another heat.

Alternate possibilities were Armco iron, such as that
used by Stone[12], or decarburized SAE 1008 steel after
Gensamer[13]. The decarburized steel was chosen for its clean-
liness as compared with the Armco iron, although the total sol-
uble impurities were much higher. The analysis of the steel
was as follows:

C	Si	Mn	P	S	Cr	Ti	Mo	Ni	Cu
0.09	0.14	0.46	0.010	0.027	0.08	0.01	0.01	0.07	0.05

Twelve tensile bars were machined to the specifications
shown in Fig. 3. The radius of curvature at the shoulder is

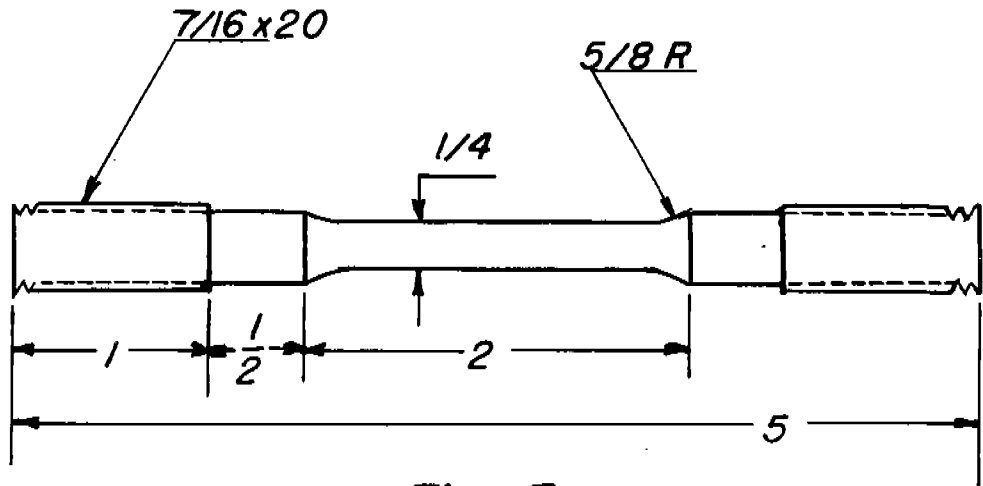7/16 x 20   5/8 R   1/4

1   1/2   2   5

Fig. 3

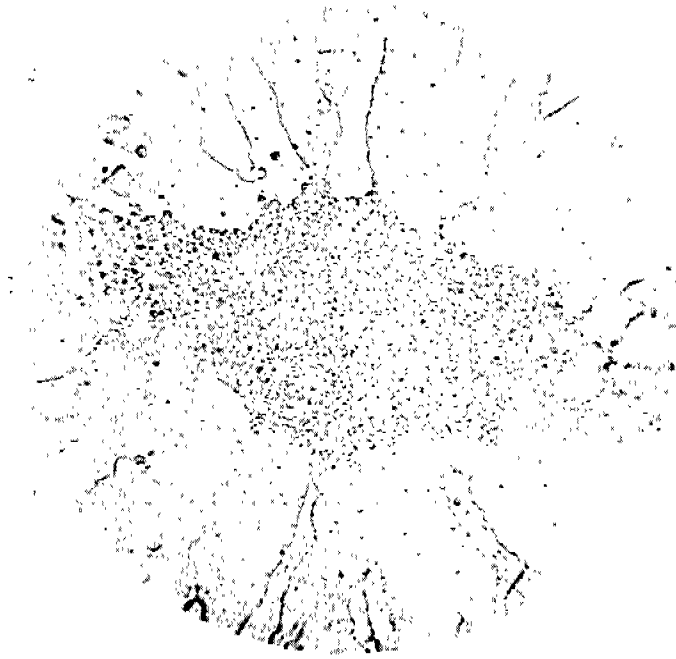S.A.E. 1008 Bar Stock as Received

Fig. 4

Fig. 5. Columnar crystals radiating from the edge
of a specimen partially decarburized in the
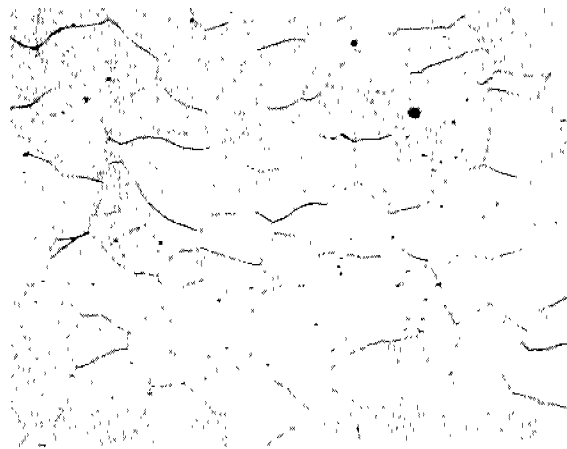region of the phase diagram. (X10)

Fig. 6. Decarburized S.A.E. 1008 stock (X100)

not shown but was 5/8 in. They were decarburized for 100 hrs.
at 720°C in hydrogen saturated with water vapor at 68°C. The
controller allowed the furnace to overshoot above 730°C, and
the specimens were decarburized in the $(\alpha + \gamma)$ phase field
resulting in a structure of columnar grains projecting from
the outside to the center of the specimens. It was realized
that the diffusion coefficient of carbon in α-iron at 720°C
is four times as great as that of carbon in γ-iron at 1000°C,

$$1000°C \quad D_\gamma^C = 2.42 \times 10^{-7} \text{ sq. cm. per sec.}$$
$$720°C \quad D_\alpha^C = 9.25 \times 10^{-7} \text{ sq. cm. per sec.}$$

but the fluctuation in line voltages at night were too un-
predictable to permit accurate control of furnace temperature.
Therefore, the temperature of 950°C was chosen as the decarburiz-
ing temperature.

The structure of the mild steel in as-received condition is
shown in Fig. 4 . The grain size is ASTM #8-9. For strain anneal
methods, the grain size should be much larger since the critical
strain increases with increasing grain size. Considering both
treatments, grain growth anneal and decarburization, the 950°C
treatment seemed most suitable.

It was found necessary to heat the specimens under a very
dry H_2 atmosphere to prevent the formation of columnar crystals
while passing through the $\alpha + \gamma$ phase region. An example of this
is shown in Fig. 5. Another reason for heating and cooling without

water saturation, is that the degree of saturation used is calculated on the basis of the iron-oxygen equilibrium at 950°C; consequently, this H_2/H_2O ratio is in equilibrium with FeO at temperatures below about 920°C and produces an oxidized surface.

The grain size was controlled by inserting a small resistance in series with the furnace at the end of the soak period. This is sufficient to decrease the current-temperature equilibrium of the furnace to about 850°C, thus giving the correct cooling rate through the α to γ transformation to produce a grain size of ASTM #2-3. The structure of the final decarburized material is shown in Fig. 6. The composition of the decarburized material was identical with that shown earlier for the bar stock, with the exception that the carbon content was reduced to 0.019%.

A series of twelve decarburized specimens were strained from 2.0% to 4.4% elongation in a one-inch gauge length in increments of 0.2%. The specimens were placed in a furnace under a dry hydrogen atomsphere and heated rapidly to 350°C. The furnace was then program-heated at 5°F per hr. to the soak temperature of 880°C, annealed for 4 days, then furnace cooled to room temperature.

Upon removal from the furnace, the specimens were observed to have a heat etched surface showing a grain size of about ASTM #000. They were then milled longitudinally to half

diameter, polished through #000 metallographic paper and etched in a 10% nital solution. The results are shown in Fig. 7.

It can be seen from Fig. 7 that the critical strain was about 3.2%. This value was chosen, and all subsequent specimens were strained 3.2% and subjected to a similar treatment. The yield has been about 50 per cent single crystals, the remainder being almost exclusively bi-crystals, with one or two tri-crystals. Milling the specimens would, of course, ruin them for further testing, so a procedure was developed for detecting the "single-crystalness" of the treated specimens. Upon removal from the growth anneal, the specimens were electropolished and etched repeatedly until a structure different from the false surface structure became apparent. Specimens showing a single crystal extending from one shoulder of the specimen to the other were electropolished and etched until no "grain islands" appeared on the surface, then given a final polish to prepare the surface for optical and X-ray examination.

Brick and Vogel[11] used an 880°C anneal in purified helium subsequent to a metallographic polish to produce a suitable surface. The present authors tried this but discarded it in favor of the electropolish method when it was found that the annealing treatment gave the same undistorted Laue photograms and slip line characteristics. The advantage
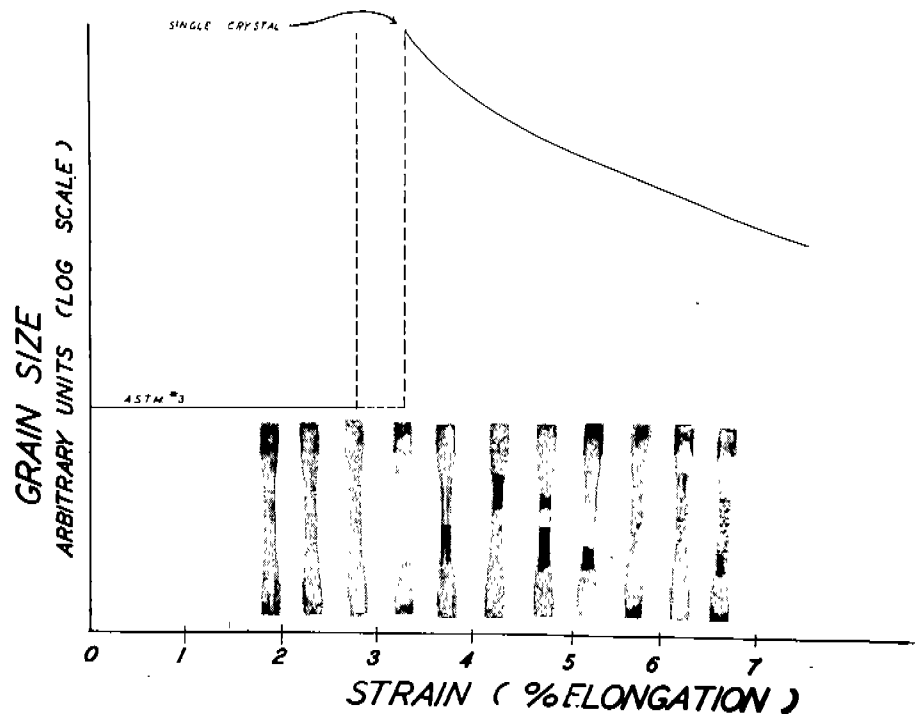
Fig. 7. Results of experiments to determine the
critical deformation to produce single
crystals of decarburized S.A.E. 1008

of the anneal method is to lower the inclusion loss from the surface. Electrolytic methods create galvanic attack at the metal-inclusion interface which make the inclusions "pop out" during polishing. This was not believed to be of serious consequence in the type of measurements to be made, and since the electropolishing is much easier, it was used in all subsequent preparations.

The orientation of all specimens was determined by Laue back-reflection methods using tungsten radiation. Sharp clear spots were obtained in all cases, thereby confirming the unstressed nature of the surface.

The tensile tests were performed on a Dillon chain driven tensile machine of 5,000 lbs. capacity. The load was measured with a Baldwin-Southwark type U-1, SR-4, load cell exciting the input circuit of a Sanborn strain gauge amplifier and recorder. This system produces a record of load versus time.

The strain was measured by means of a specially constructed strain gauge employing two linear differential transformers which are connected to a parallel compensated Schaevitz recorder. This apparatus records elongation versus time. It would have been most desirable to have an X-Y recorder with one axis load and the other strain, but unfortunately, this piece of equipment was unavailable at the time. The load-time curves are

sufficient to show the yield point in most crystals, although autographic load-elongation curves would be much better.

An insulated container surrounded the specimens at all temperatures and contained the various media used to obtain the test temperature. The cooling media are listed below:

$+200^\circ C$ - Russian mineral oil

$+100^\circ C$ - Boiling water

Room Temp.- Stagnant air

$0^\circ C$ - Ice + water mixture

$-70^\circ C$ - Dry ice + acetone mixture

$-196^\circ C$ - Liquid nitrogen

The specimens were protected by a coating of rubber cement to prevent scratching and corrosion by the temperature medium. This coating was easily stripped off after testing and retained the electropolished surface very well.

Measurements of the traces of slip and twin markings were made on a special goniometer head similar to that described by Brick and Vogel[11]. This goniometer is the same one used to align the specimen for the Laue pictures and prevents errors in angular measurement when the specimen is transferred from one goniometer to another. The goniometer was attached to the rotating head of a Bausch

and Lomb research metallograph and locked in position by a thumb screw. Measurements of the angle of inclination of the glide plane to the specimen axis were made at 10°. intervals around the specimen.
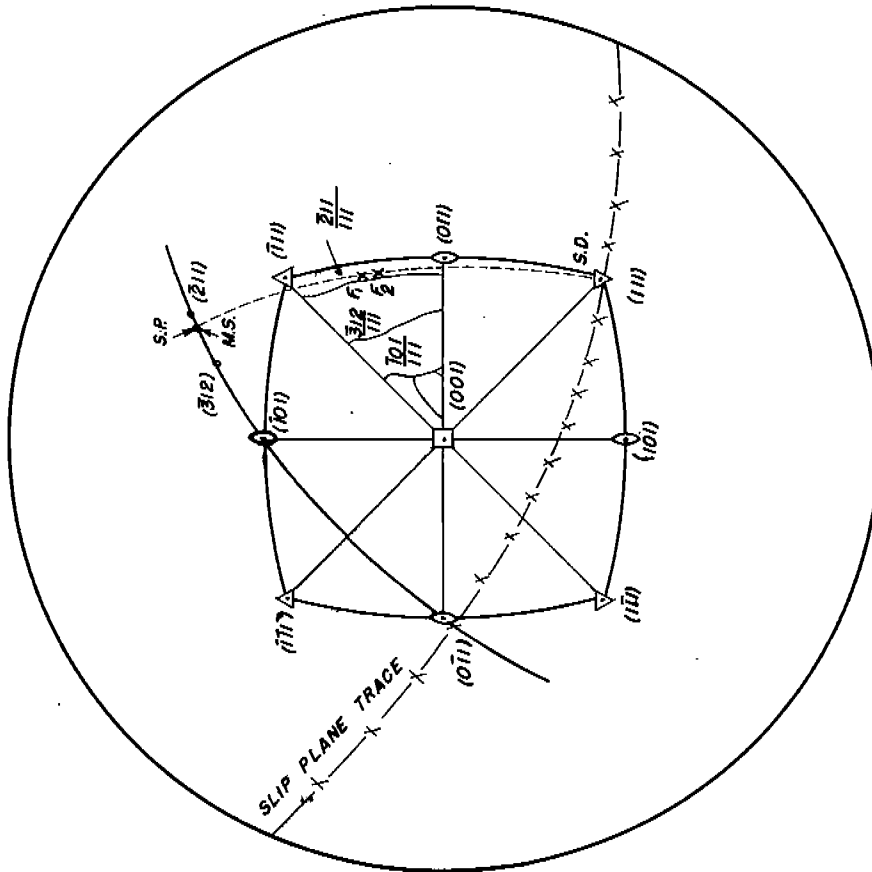
The angular measurements were plotted stereographically and were found to fall on a great circle with errors less than 4 to 5 degrees in the worst cases. The pole of this great circle was the pole of the particular glide plane. In all cases the over-all orientation of the glide ellipse was measured and hereinafter will be called the integrated glide ellipse.

Experimental Results

Geometrically the problem of determining a critical resolved shear stress consists very simply of obtaining a yield stress and resolving it into a given plane in space-- the space being the specimen itself. The complexities arise from the experimental determinations of the yield stress, the plane of glide or twinning or cleavage, and the direction lying in that plane.
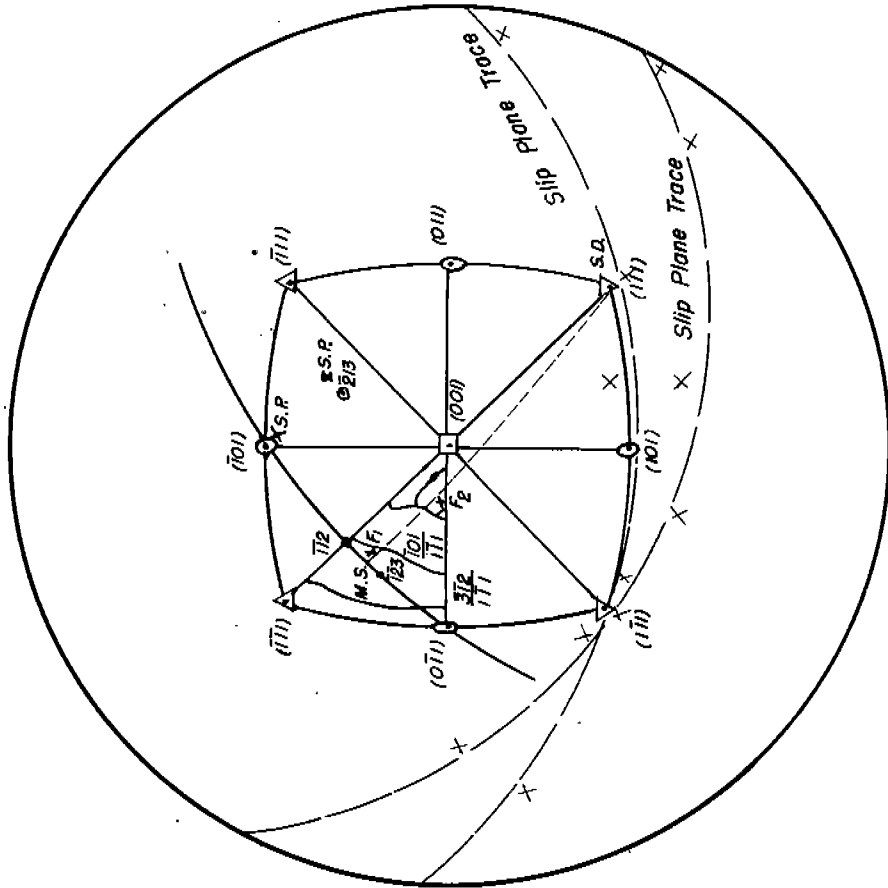
The Slip Plane

Figs. 8 to 20 show the orientations of all crystals referred to the standard (001) projection, while Fig. 21 summarizes the relative positions of the maximum shear

Projection of Specimen A-7

F₁F₂ Specimen Axis Before and After Deformation.
M.S. Pole of Maximum Shear Plane Containing (lll)
S.P. Pole of Slip Plane
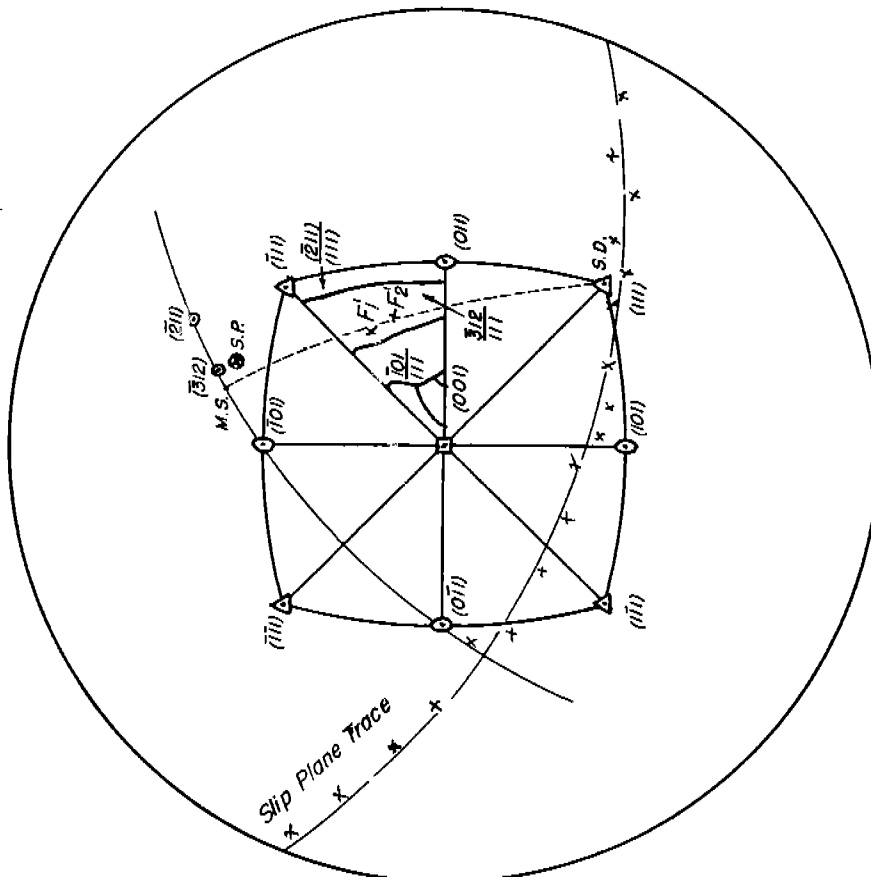S.D. Slip Direction

Fig. 9
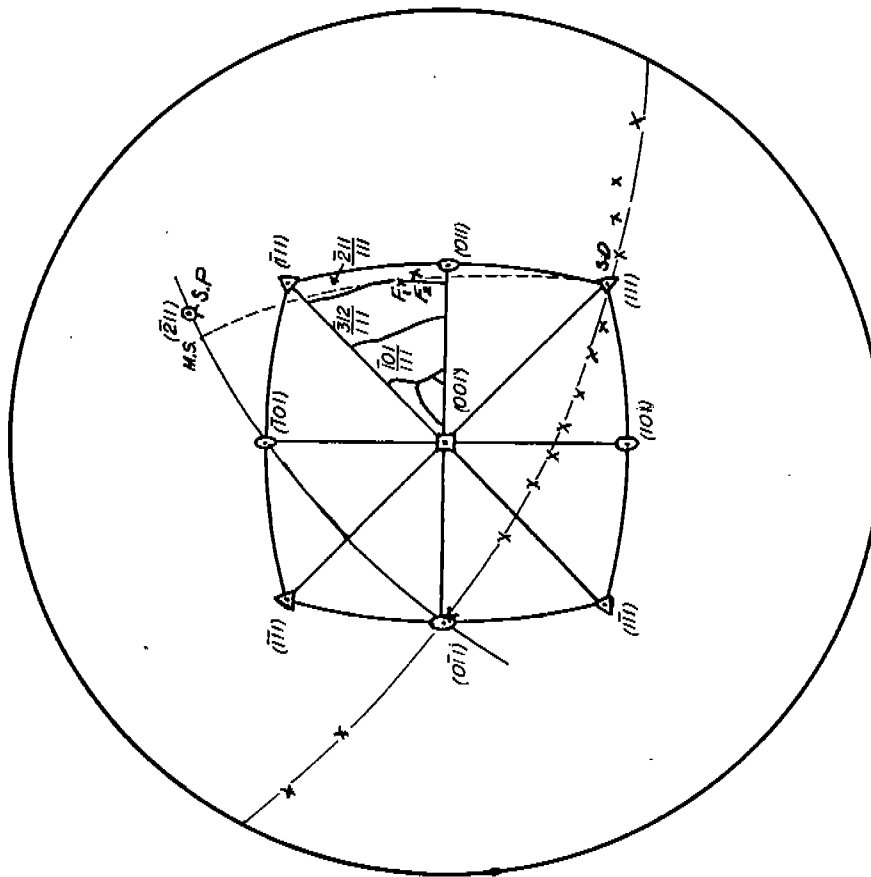

Projection of Specimen Br-2

F₁F₂ Specimen Axis Before and After Deformation
M.S. Pole of Maximum Shear Plane Containing (lll)
S.P. Pole of Slip Plane
S.D. Slip Direction

Fig. 8

Projection of Specimen A-3

F_1', F_2' Specimen Axis Before and After Deformation.
M.S. Pole of Maximum Shear Plane Containing (III).
S.P. Pole of Slip Plane.
S.D. Slip Direction.

Fig. 11

Projection of Specimen A-1

F_1, F_2 Specimen Axis Before and After Deformation
M.S. Pole of Maximum Shear Plane Containing (III)
S.P. Pole of Slip Plane
S.D. Slip Direction

Fig. 10

Projection of Specimen A—4

F'_1, F'_2 Specimen Axis Before and After Deformation.

M.S. Pole of Maximum Shear Plane Containing (111).

S.P. Pole of Slip Plane.

S.D. Slip Direction.

Fig. 13

Projection of Specimen A—5

F'_1, F'_2 Specimen Axis Before and After Deformation.

M.S. Pole of Maximum Shear Plane Containing (111).

S.P. Pole of Slip Plane.
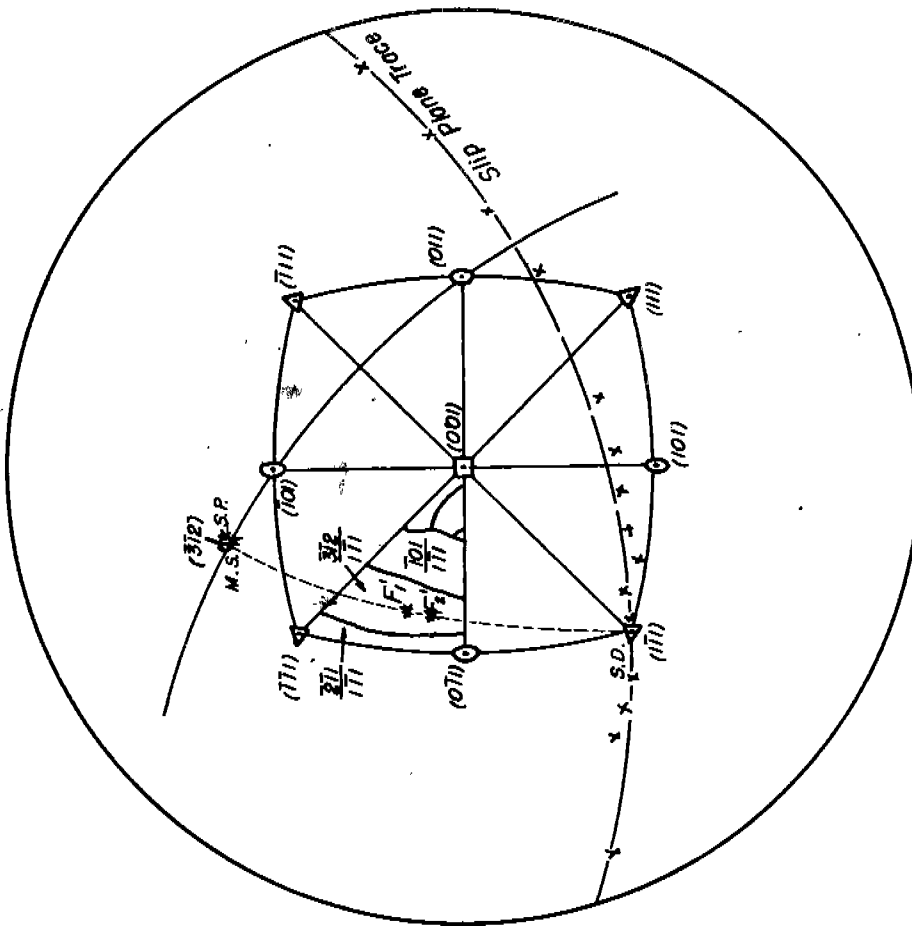
S.D. Slip Direction.

Fig. 12

Projection of Specimen A-6

$F'_1 F'_2$ Specimen Axis Before and After Deformation
M.S. Pole of Maximum Shear Plane Containing (111)
S.P. Pole of Slip Plane
S.D. Slip Direction

Fig. 15

Projection of Specimen A-12

$F_1 F_2$ Specimen Axis Before and After Deformation.
M.S. Pole of Maximum Shear Plane Containing (111)
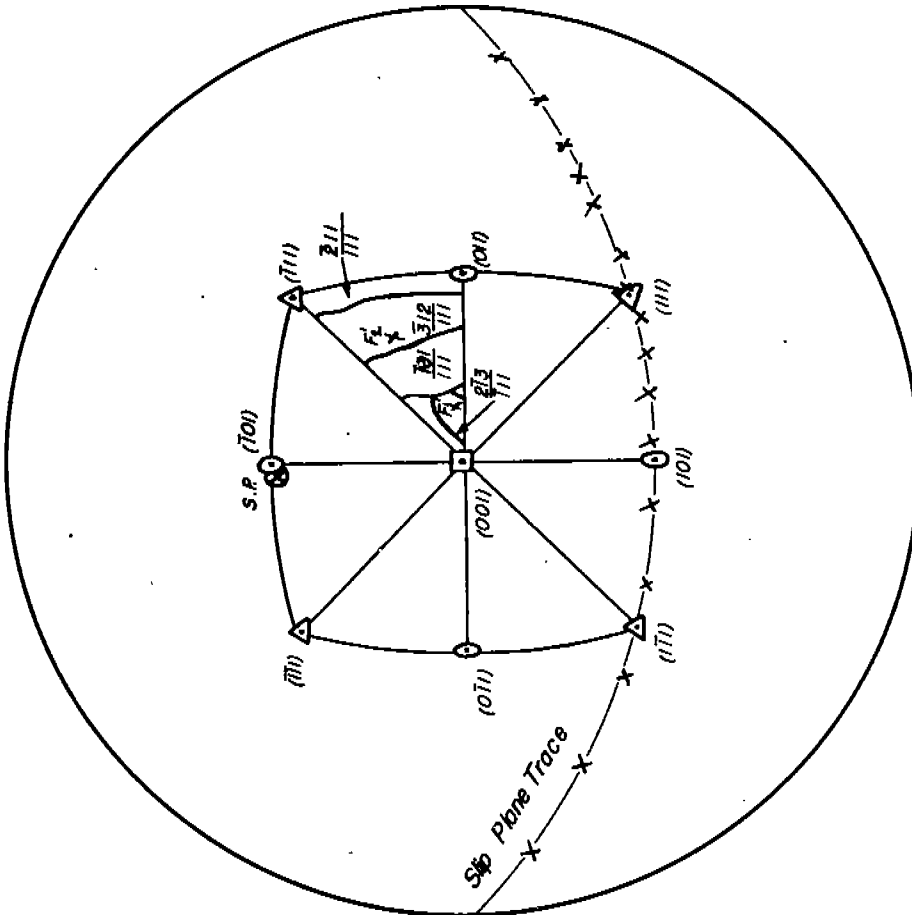S.P. Pole of Slip Plane.
S.D. Slip Direction.

Fig. 14

Projection of Specimen A-9

$F_1'F_2'$ Specimen Axis Before and After Deformation.
M.S.   Pole of Maximum Shear Plane Containing (111).
S.P.   Pole of Slip Plane.
S.D.   Slip Direction
T.P.   Pole of Twin Plane

Fig. 17

Projection of Specimen A-6

F_1F_2' Specimen Axis Before and After Deformation
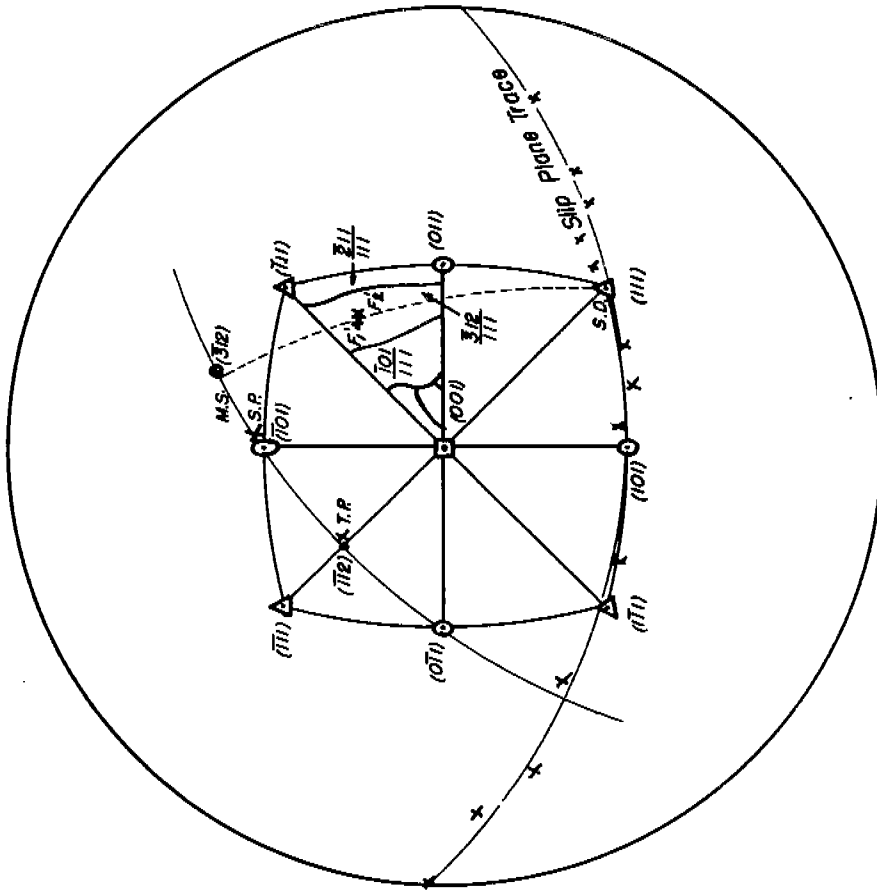T.P.   Pole of Twin Plane
T.D.   Twin Direction

Fig. 16

Projection of Specimen A-11

$F_1'F_2'$ Specimen Axis Before and After Deformation.
M.S. Pole of Maximum Shear Plane Containing (111)
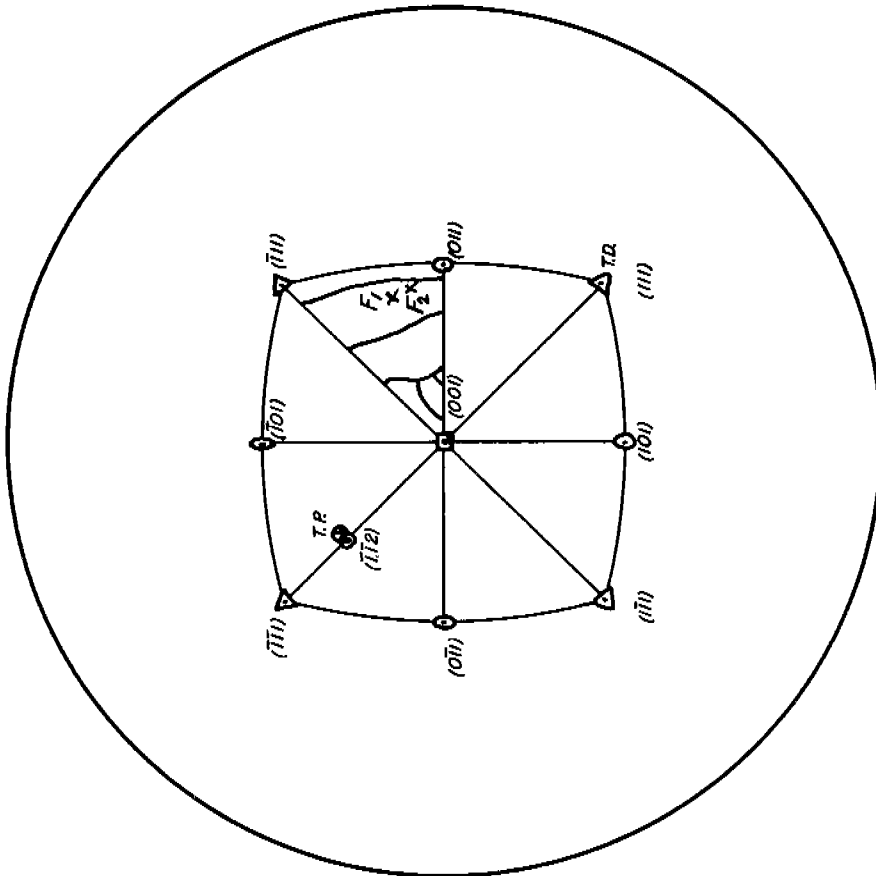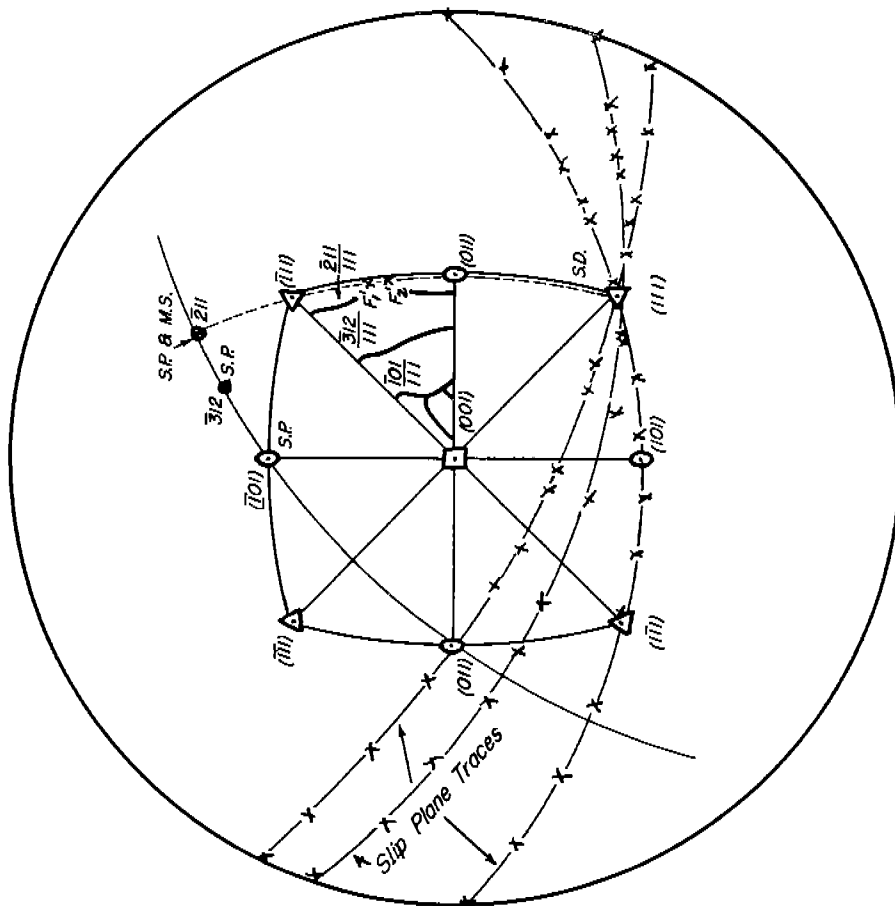S.P. Pole of Slip Plane
S.D. Slip Direction.

Fig. 19

Projection of Specimen A-11

$F_1 F_2$ Specimen Axis Before and After Deformation.
M.S. Pole of Maximum Shear Plane Containing (111)
T.P. Pole of Twin Plane.
T.D. Twin Direction.

Fig. 18

Relative Positions of Maximum Shear Stress Poles (·)
and Glide Plane Poles (x).

Specimen Number	Slip Direction	Tempera-ture °C									
Br-2	(111)	+195°									
A-7	—	+98°									
Br-3	(1̄11)	+25°									
A-1	(111)	+31°									
A-3	(111)	0°									
A-5	(1̄11)&(111)	0°									
A-4	(11̄1)	-73°									
A-12	(111)	-70°									
A-6	(11̄1)	-196°									
A-9	(111)	-196°									
A-11	(111)	-196°									

Fig. 21

Fig. 20

Projection of Specimen Br-3

F₁'F₂'   Specimen Axis Before and After Deformation.
M.S.   Pole of Maximum Shear Plane Containing (111).
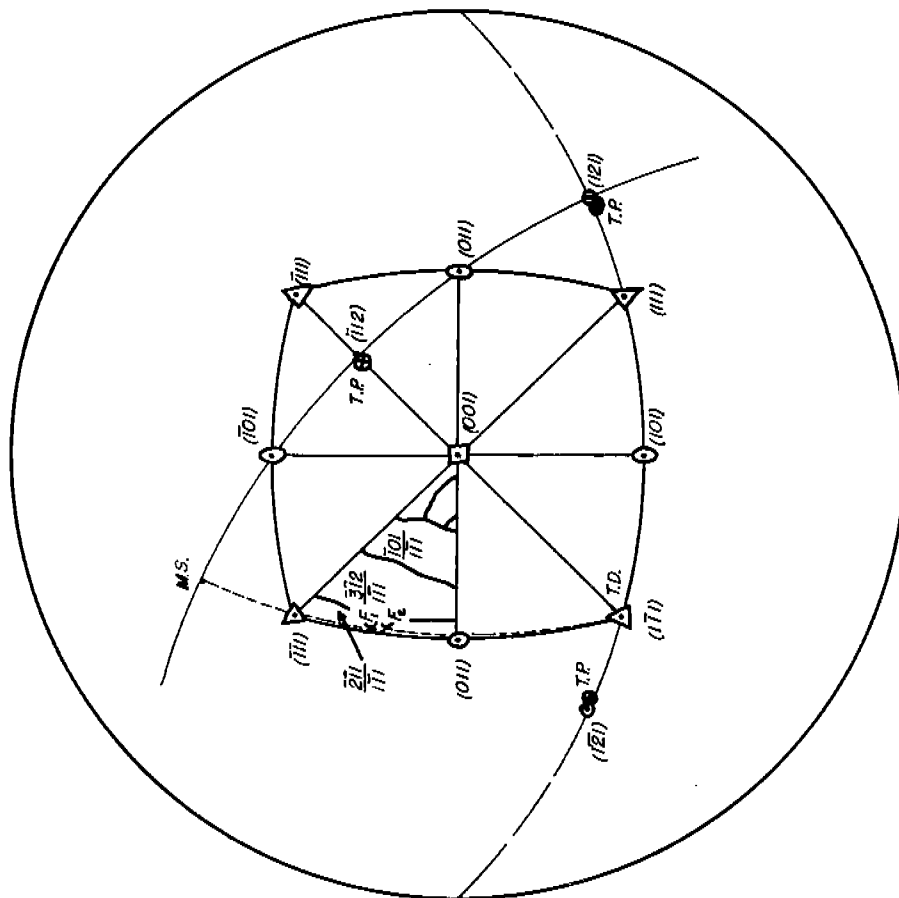S.P.   Pole of Slip Plane.
S.D.   Slip Direction.

stress planes and the glide planes for all the specimens. The plane of maximum shear stress is determined stereographically by drawing a great circle through the poles of the specimen axis (F_1, F_2) to the point where it intersects the [111] zone. This intersection (MS) is the pole of the maximum shear stress plane. This great circle is terminated on the other end by the slip direction (SD).

From Fig. 21, it can be seen that at low temperatures the slip plane is always inclined toward and usually coincides with the ($\bar{1}01$) plane. In specimen A-11 three sets of planes were visible; however, the ($\bar{1}01$) plane was most prominent. At higher temperatures it appears that the glide plane is inclined toward the nearest low index plane (110), (112), or (123). No maximum shear stress plane is indicated for specimens A-7 and A-5 because the slip direction is not clearly indicated. Specimen BR-3 does not follow either trend and cannot be accounted for at the present time. In all cases, except that of BR-3, the pole of the integrated glide ellipse lies close enough to either a (110), (112), or (123) plane to be considered as having that orientation.

The Slip Direction

The method of Fahrenhorst and Schmid was used to determine the slip direction--that of extrapolating the great circle drawn through the poles of the specimen axis before

and after deformation. In eight of the ten specimens, the
slip direction was clearly the [111] . Specimens A-5 and
A-7 gave complex results, but they are to be expected when
the specimens are located near two possible slip planes
not having a common slip direction.

The Yield Point

Sharp inhomogeneous yield phenomena were not observed
in all specimens although the analyses showed 0.012% carbon
to be present. Figs. 26 to 35 show the load-time curves for
each crystal. The scale of load is not indicated on each
chart, for it varies with adjustment of the sensitivity of
the recorder; but each curve is referred to a standard
calibration chart and the load computed from there. Specimens
A-12, A-1, A-3, BR-3, and A-4 show what might be called double
yielding. At least there is a leveling off of the curve after
the initial change in slope.

Specimens A-11, A-9, and A-6 were strained at -196°C and
exhibited twinning as the principal mode of deformation.
There is no change in slope of the load-time curve for such
a case but merely a sudden drop in load accompanied by a loud
"bang" followed by an increase in load parallel to the original
curve before twinning. The large breaks in the curves are
caused by a change in scale of the recording apparatus. Al-
though the strain was measured over the entire reduced section
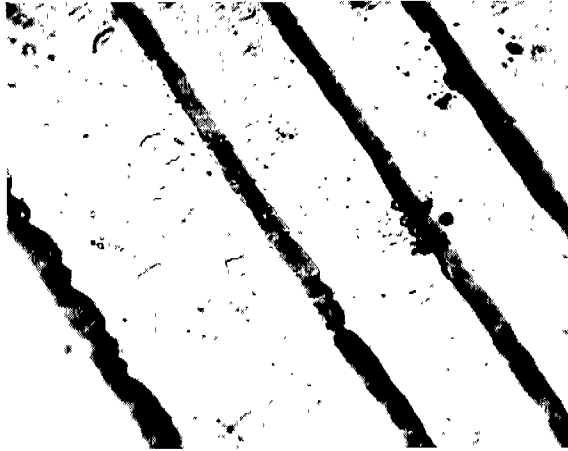of the test bar, no cases could be found where the strain

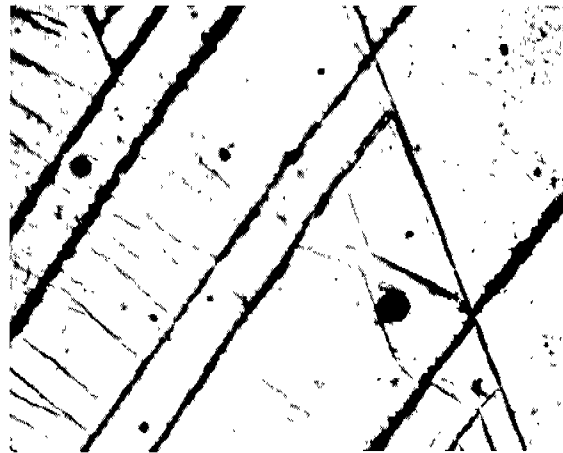Fig. 22a.   Twins and slip lines in specimen A-11 (X1000)

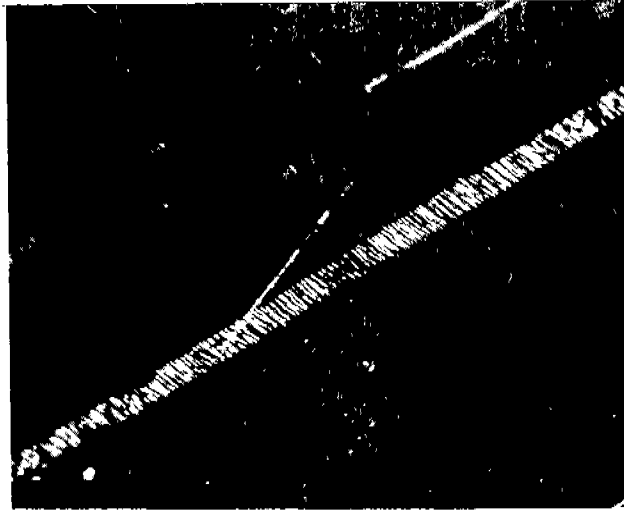Fig. 22b.   Twins and slip lines in specimen A-11 (X150)

Fig. 23. Slip lines appearing in scratch parallel
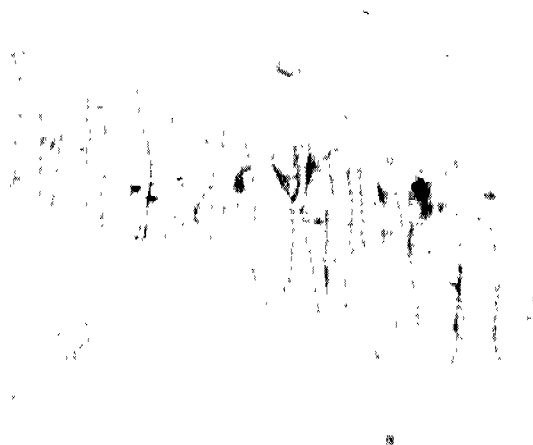to compression axis of single crystal
(X 150) Polarized Light.

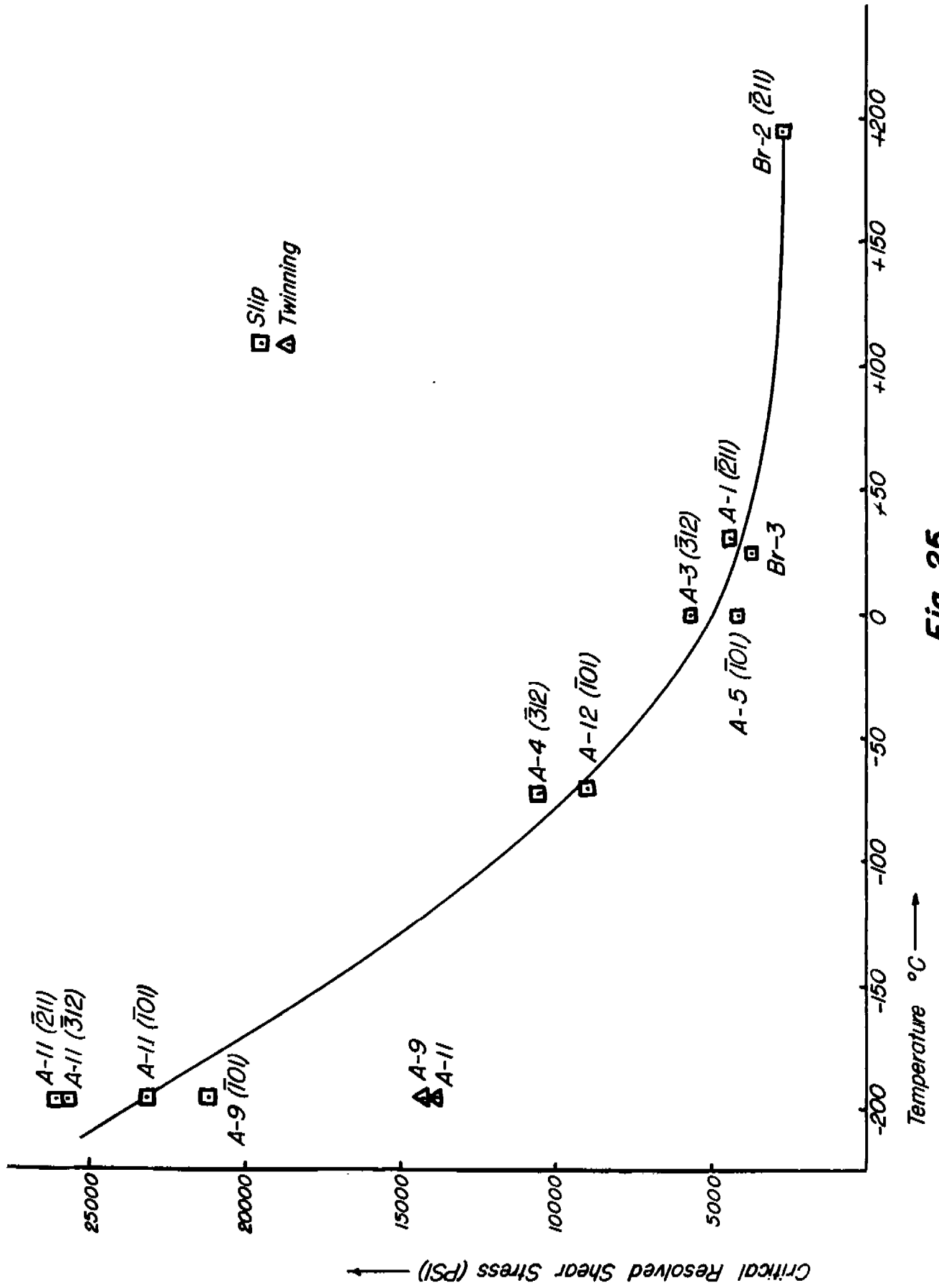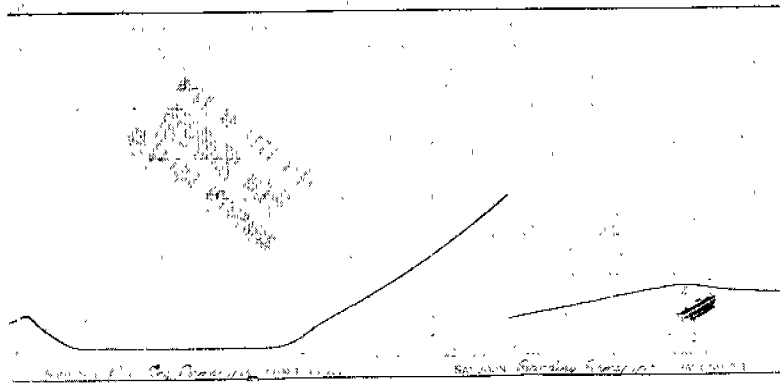Fig. 24. Same as Fig. 23 but vertical
illumination (X 1000)

Fig. 25

Fig. 26. Load (vertical) versus time curve for
specimen A-4 strained at -73°C.

Fig. 27. Load (vertical) versus time curve for
specimen A-6 strained at -196°C.

Fig. 29. Load (vertical) versus
time curve for specimen
A-3 strained at 0°C.

Fig. 31. Load (ordinate) versus
time curve for specimen
A-1 strained at 31°C.

Fig. 28. Load (vertical) versus time
curve for specimen Br-3 strained
at 25°C.

Fig. 30. Load (ordinate) versus time
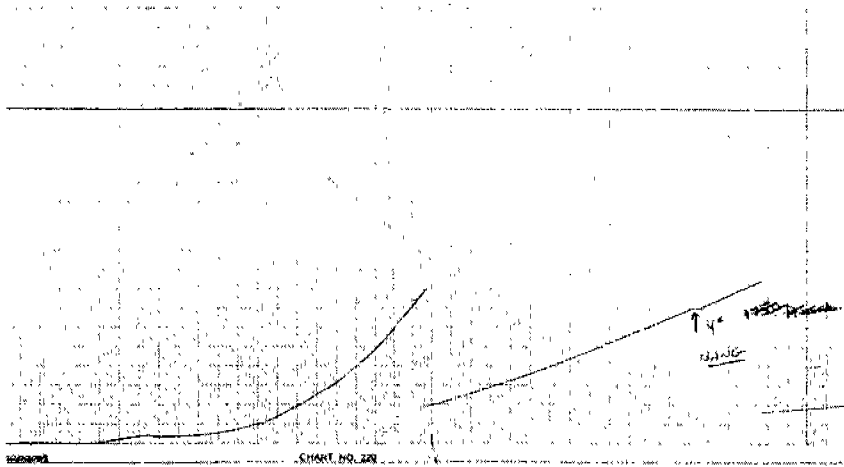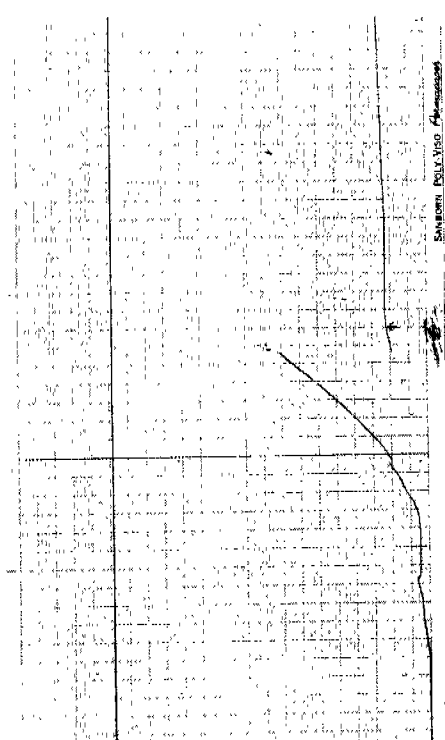curve for specimen A-9
strained at -196°C.

Fig. 32.   Load (vertical) versus time
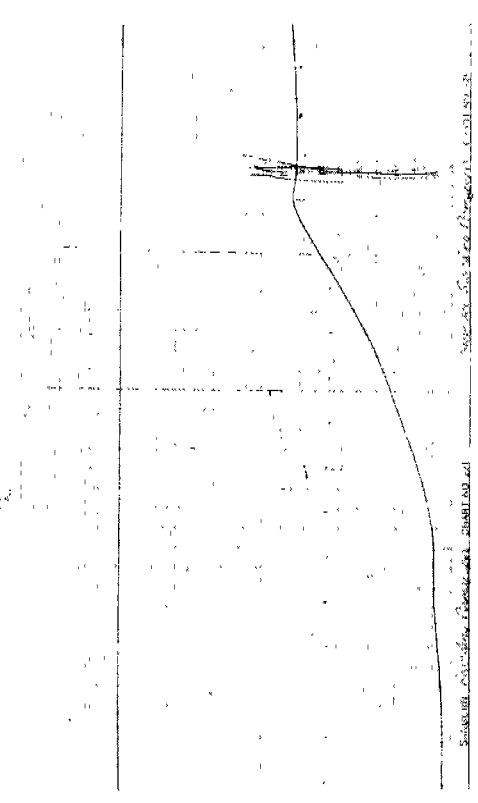curve for specimen A-5 strained
at 0°C.

Fig. 33.   Load (vertical) versus
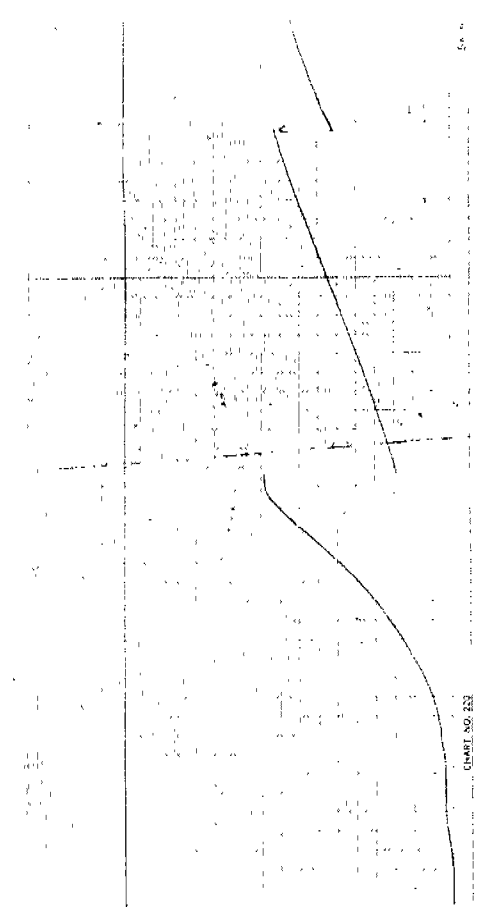time curve for specimen
A-12 strained at -70°C.

Fig. 34.   Load (ordinate) versus time
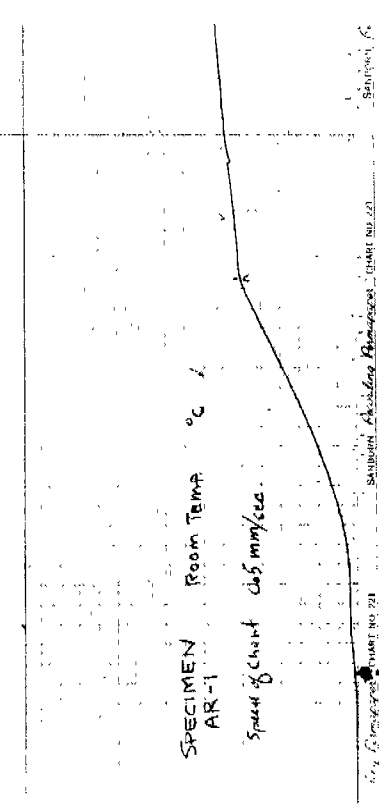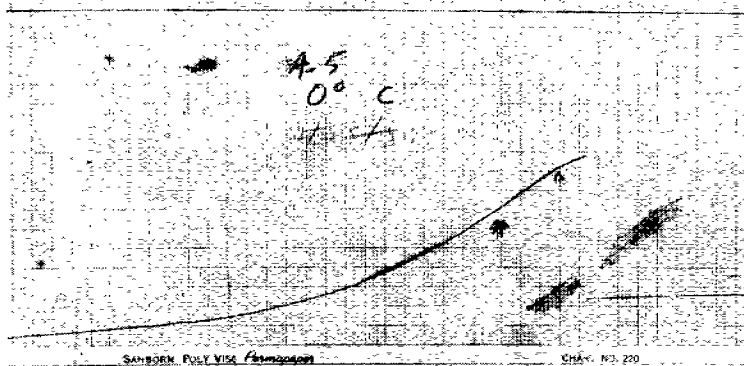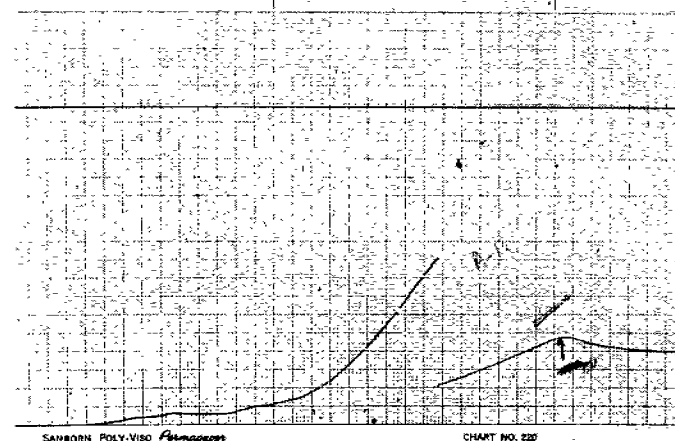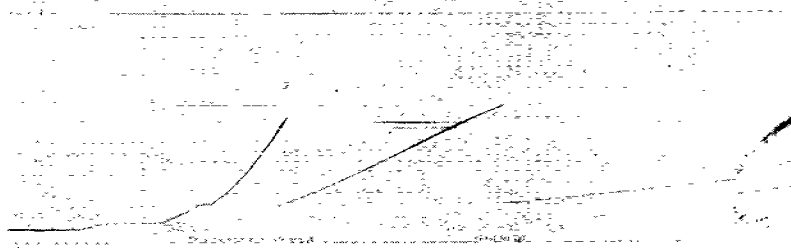curve for specimen A-11 strained
at -196°C.
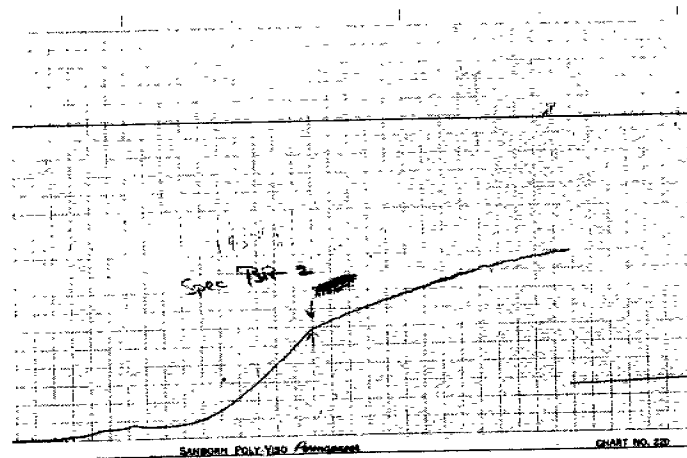
Fig. 35.   Load (ordinate) versus
time curve for specimen
Br-2 strained at 195°C.

occurred preferentially along the crystal. Something resembling Lüders bands were observed on the specimens pulled at room temperature and 0°C, but the strains were not high enough to permit definite conclusions to be made concerning this.

The Nature of Slip and Twin Traces

The most difficult part of this investigation is the observation and measurement of the traces of the glide or twin planes. At low deformations such as 2-4%, the slip lines appear as very faint striations on the surface and can only be seen at certain magnifications and under certain lighting conditions. This is particularly true for specimens tested between -70°C and +30°C. At higher or lower temperatures, they seem to be more visible. As in previous investigation the slip lines were found to vary in linearity and forkedness with position relative to the slip direction.

When in one specimen it was observed that slip lines were much more visible in a scratch on the specimen, a special single crystal was deliberately scratched with a diamond and deformed in compression. The results are shown in Figs. 23 and 24. Within the scratch the lines are broad and distinct but are nowhere else visible. This is in agreement with Paxton et al.[14] that mechanical deformation of the surface increases the visibility of the lines and changes their appearance from a striated one to a series of discrete steps.

Electron Microscope and Interferometric Studies

No results from the electron microscopy studies are available at this time except to say that replicas of a smooth unstrained surface of the crystals have been satisfactorily prepared. It is hoped that very soon some results on the nature of the slip lines at high resolving powers will be forthcoming.

Preliminary experiments on the Tolansky interferometer indicates the height differences between the lines shown in Figs. 24 and 25 is approximately 300-500 $\overset{o}{A}$. The technique must be further refined before quantitative results will be available.

Critical Stresses for Slip and Twinning

Table I and Fig. 25 show the results of attempts to calculate the critical resolved shear stresses for slip and twinning. The scatter between duplicate specimens is quite small and well within the expected error. The constancy predicted by critical resolved shear stress law seems to be fairly well obeyed.

Critical stresses for twinning are recorded for two specimens, A-9 and A-11. These values are also quite similar. In these specimens, it was not possible to determine whether slip or twinning occurred initially since traces of both were found. Photomicrographs of specimen A-11 are shown in Figs. 22(a) and (b). An unmarked specimen tested at -196°C showed

TABLE I

Specimen No.	Test Temp.,°C	Slip Plane	Critical Resolved Shear Stress on				
			Slip Plane	MSS Plane	(101)	(123)	(112)
BR-2	195	(211)	2735	2735	2432	2735	2735
A-7	98	(101)	--	--	--	--	--
BR-3	25	(?)	3786	4017	4017	4017	3941
A-1	31	(211)	4411	4411	4023	4411	4336
A-3	0	(312)	5676	5484	5414	5484	5275
A-5	0	(101)	4146	--	4146	--	--
A-4	73	(312) (110)	10570	10570	10070	10570	10410
A-12	70	(101)	9000	9173	8825	9000	8646
A-6	196	(101)	17270	18530	17270	18530	18220
A-9	196	(101)	21200	21690	20690	21690	21200
A-11	196	(101) (312) (211)	23150 25800 26150	26150	23150	25800	26150

no slip lines when removed immediately after yielding.

Discussion

The position of the integrated glide ellipse in iron
is found to follow two distinct patterns. At -70°C and
below, the pole of the integrated ellipse coincides with a
(110) pole regardless of the orientation of the crystal and
the plane of maximum shear stress. Although traces of (112)
and (123) planes appear at low temperatures, the (110) trace
is most prominent. In each case, except that of BR-3, the
pole of the glide ellipse lies close enough to one of the
three low index planes of the [111] zone to say that the
slip is crystallographic on a macroscopic or average basis.
But does this have significance? In certain aspects, yes,
in that it allows the stress on this integrated plane of
glide to be calculated and a curve of critical stress for
slip to be plotted as a function of temperature. Funda-
mentally, though, we are measuring the position of a non-
entity. The integrated glide plane is a hypotetical one
consisting of the best straight line than can be drawn
through a series of forked and wavy lines. By definition
it is not a plane.

On the other hand, the concept of the integrated
ellipse is not altogether useless. It enables a rough

sketch of the deformation picture to be made from various combinations of planes and directions. Essentially all the experiments on deformation of single crystals of iron have revealed the same data that:

1. Slip line traces are forked and wavy and that the waviness varies with respect to the slip direction.

2. The position of the integrated glide ellipse may occupy any position in the [111] zone and may or may not coincide with the maximum shear stress plane.

3. Lower temperatures favor slip on the (110) type planes.

4. The twinning plane is definitely the (112).

Any of the proposed theories explain some of the observations but not others. A theory of combined slip on various planes could, with a little evasiveness of tongue, explain all the observations. The problem remains to find a measuring stick capable of resolving the atomic nature of slip and then, starting from that point, to construct a theory of deformation for the body-centered-cubic lattice.

Twinning was predominant in specimens A-11, A-9, and A-6. It would be desirable to determine whether twinning occurred before, after, or during slip; but so far this has not been possible. If twinning occurs simultaneously with slip, this will indeed be difficult to detect. Critical resolved shear

stress appears to be the criterion for twinning, but the data
are not complete enough to make this conclusion a definite one.

Certain effects on the appearance of slip lines as af-
fected by surface condition are found to be of interest. Me-
chanical deformation of the surface changes the markings from
fine striations to coarse discrete lines which appear at much
lower strains. This is in accord with the work of Paxton, who
showed that mechanical polishing of a single crystal increased
the visibility of slip lines as compared with those on an
electropolished surface. The problem remains as to which of
the two structures is the true one. One would suppose that
the striated appearance of the electropolished and supposedly
undeformed surface is the true effect, and yet this striated
appearance is peculiar to the body-centered lattice. The
markings found on mechanically polished surfaces or in
scratches on electropolished surfaces are more like those
found in metals of other crystal structures, although they
are forked and wavy. When results are complete on the
electron microscope and interferometric studies, perhaps
more can be said concerning the effect of surface con-
dition upon the nature of the slip markings.

Fig. 36 shows a Laue photogram after deformation. The
phenomenon to be noted here is the separating of spots into
three or four discrete layers. This is similar to observa-
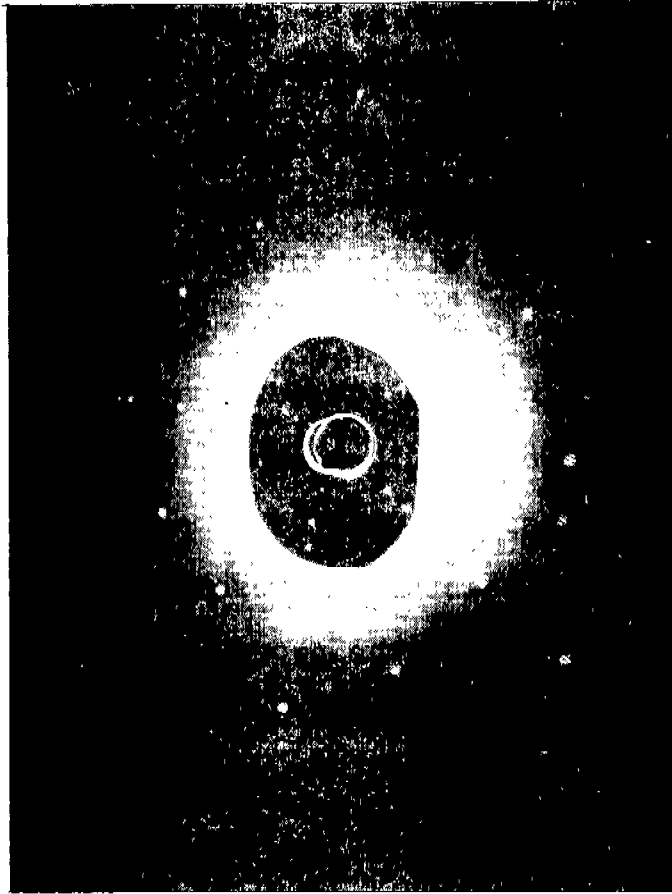tions made on polygonization in recrystallized metals and

Fig. 36. Laue photogram of specimen A-1
after 4% strain, showing the
splitting of spots.

may perhaps be due to a "polygonal" lattice of slight misfit caused by the deformation. This is pure speculation and the answer is not known, but it is included for curiosity's sake.

Future Work

The results obtained thus far in this investigation are perhaps too scant to confirm any one theory of slip or twinning. Further tensile data above -70°C should help to define the behavior of the integrated glide ellipse as a function of temperature and orientation but will probably not obtain insight into the deformation mechanism on an atomic scale. On the other hand, the electron microscope and interferometer may uncover some interesting points on the atomic or at least submicroscopic mechanism.

The other part of the program which needs investigation is that of the slip to twinning transition. Here the difficulties should be only experimental in nature. To obtain constant temperature baths in suitable intervals from -70°C to -196°C is a very difficult problem. Elaborate and expensive refrigeration systems are completely out of the question. Perhaps some cooling system involving liquid nitrogen circulating through coils immersed in a suitable liquid would be satisfactory.

The study of cleavage is even more difficult from an experimental standpoint. The three specimens tested at

-196°C have shown no cleavage and this was expected since no (001) planes were suitably oriented. In fact only two or three crystals have an orientation that places a (100) pole close to the specimen axis. Perhaps even in these specimens, cleavage will not occur at -196°C. If not, then the temperature must be drastically lowered to liquid hydrogen or liquid helium. Both of these coolants are not ideally suited since hydrogen is explosive and helium is almost prohibitively expensive.

There are then three possible places upon which to concentrate effort for the closing six months of this project:

1. Slip:

> Test several specimens of varying orientation between -70°C and +200°C with the hope of finding a regular variation to the behavior of the glide ellipse.

2. Twinning :

> a. Construct a suitable cooling apparatus to obtain temperatures from -70°C to -196°C.

> b. Test several specimens in this temperature range to determine (1) at what temperature twinning begins; (2) does slip precede, accompany, or follow twinning below the temperature found in (1); and (3) whether twinning can be correlated with a critical resolved shear stress theory.

3. <u>Cleavage</u> :

    a. To obtain a cooling medium that will promote cleavage in any specimen regardless of orientation.

    b. To calculate a fracture stress curve for single crystals of iron.

    c. To verify the critical normal stress theory of cleavage for iron.

With each of these investigations, a concurrent study of the submicroscopic nature of slip would be carried out with specimens already strained; that is, no crystals would be "wasted" on such an investigation.

Bibliography

1. G. I. Taylor and C. F. Elam, _Proceedings Royal Society of London_, Volume A112, (1926), p. 337.

2. G. I. Taylor, _Proceedings Royal Society of London_, Volume A118, (1928), p. 1.

3. N. Fahrenhorst and E. Schmid, _Zeitschrift für Physik_, Volume 78, (1932), p. 383.

4. C. S. Barrett, G. Ansel, and R. F. Mehl, _Trans. Amer. Soc. Metals_, Volume 25, (1937), p. 702.

5. C. S. Barrett, _Structure of Metals_, McGraw-Hill, New York.

6. E. W. da. C. Andrade, _Proceedings Physical Soc._, Volume 52, (1940), p. 1.

7. R. Smoluchowski, Discussion to Chen and Maddin article, _Journal of Metals_, 1952.

8. A. J. Opinsky and R. Smoluchowski, _Journal Applied Physics_, Volume 22, (1951), p. 1428.

9. A. J. Opinsky and R. Smoluchowski, Doctorate Dissertation, Carnegie Institute of Technology, 1950.

10. N. K. Chen and R. Maddin, _Trans. Amer. Inst. Mining & Met. Engrs._, Volume 191, (1951), p. 937.

11. F. L. Vogel, Jr., and R. M. Brick, Univ. of Pennsylvania Technical Report #1 to Flight Research Lab., Wright-Patterson Air Force Base.

12. F. G. Stone, _Trans. Amer. Inst. Mining and Met. Engrs._, Volume 175, (1948), p. 908.

13. M. Gensamer and R. F. Mehl, _Trans. Amer. Inst. Mining and Met. Engrs._, Volume 131, (1938).

14. H. Paxton, Private communication. To be published, University of Birmingham, England.